Bioresource Technology 270 (2018) 359–367

Contents lists available at ScienceDirect

Bioresource Technology

journal homepage: www.elsevier.com/locate/biortech

Biokinetics of microbial consortia using biogenic sulfur as a novel electron donor for sustainable denitrification

Anastasiia Kostrytsia[a,*], Stefano Papirio[b], Liam Morrison[c], Umer Zeeshan Ijaz[d], Gavin Collins[e], Piet N.L. Lens[c,f], Giovanni Esposito[a]

[a] Department of Civil and Mechanical Engineering, University of Cassino and Southern Lazio, via Di Biasio 43, 03043 Cassino (FR), Italy
[b] Department of Civil, Architectural and Environmental Engineering, University of Naples Federico II, via Claudio 21, 80125 Naples, Italy
[c] Earth and Ocean Sciences, School of Natural Sciences and Ryan Institute, National University of Ireland Galway, University Road, Galway H91 TK33, Ireland
[d] School of Engineering, University of Glasgow, Glasgow G12 8LT, United Kingdom
[e] Microbial Communities Laboratory, School of Natural Sciences and Ryan Institute, National University of Ireland Galway, University Road, Galway H91 TK33, Ireland
[f] UNESCO-IHE, Institute for Water Education, PO Box 3015, 2601 DA Delft, The Netherlands

GRAPHICAL ABSTRACT

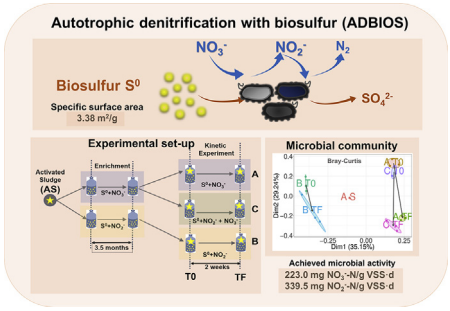

ARTICLE INFO

Keywords:
Autotrophic denitrification
Biogenic sulfur
Nitrite accumulation
Biokinetics
Community structure

ABSTRACT

In this study, the biokinetics of autotrophic denitrification with biogenic S^0 (ADBIOS) for the treatment of nitrogen pollution in wastewaters were investigated. The used biogenic S^0, a by-product of gas desulfurization, was an elemental microcrystalline orthorhombic sulfur with a median size of 4.69 μm and a specific surface area of 3.38 m^2/g, which made S^0 particularly reactive and bioavailable. During denitritation, the biomass enriched on nitrite (NO_2^-) was capable of degrading up to 240 mg/l NO_2^--N with a denitritation activity of 339.5 mg NO_2^--N/g VSS·d. The use of biogenic S^0 induced a low NO_2^--N accumulation, hindering the NO_2^--N negative impact on the denitrifying consortia and resulting in a specific denitrification activity of 223.0 mg NO_3^--N/g VSS·d. Besides *Thiobacillus* being the most abundant genus, *Moheibacter* and *Thermomonas* were predominantly selected for denitrification and denitritation, respectively.

1. Introduction

The increased depletion of resources, the rising water stress, the need of decreasing the carbon footprint and the stringent nutrient discharge limits encourage the development of new bioprocesses for nitrogen removal from wastewater. Conventionally, nitrate (NO_3^-) and nitrite (NO_2^-) reduction is coupled to the oxidation of organic matter by heterotrophic microorganisms in wastewater treatment plants

* Corresponding author.
E-mail address: kostritsia@gmail.com (A. Kostrytsia).

https://doi.org/10.1016/j.biortech.2018.09.044
Received 1 August 2018; Received in revised form 7 September 2018; Accepted 9 September 2018
Available online 11 September 2018

(WWTPs). However, heterotrophic denitrification and denitritation typically require the supply of organic matter, resulting in higher sludge production and operational costs (Sun and Nemati, 2012).

To overcome these disadvantages, chemically synthesized elemental sulfur (S^0) has been used as a cheaper and effective electron donor for autotrophic denitrifying microorganisms treating wastewaters poor in organics (Wang et al., 2016). However, the low water solubility of chemically synthesized S^0 limits its availability to microorganisms and makes denitrification and denitritation kinetics slower than that achieved with more soluble electron donors (Kiskira et al., 2017a; Mora et al., 2015; Park and Yoo, 2009; Zou et al., 2016). Additionally, elevated NO_2^- concentrations when using chemically synthesized S^0 during autotrophic denitrification can decrease the overall process efficiency (Christianson et al., 2015; Kostrytsia et al., 2018). Specifically, the sulfur to nitrogen (S/N) molar ratio, the feed pH and the microbial community structure are known to be among the main factors controlling the NO_2^- accumulation. Therefore, it is crucial to investigate the potential of alternative electron donors for both NO_3^- and NO_2^- removal, such as biogenic S^0.

Biogenic S^0 (or biosulfur) is a biological product obtained from the incomplete oxidation of sulfide in gaseous streams under oxygen-limiting conditions by S-oxidizing microorganisms (Florentino et al., 2015). The Thiopaq® technology (Paques BV, the Netherlands) is, for instance, a well-established process aimed at the biological gas desulfurization that integrates hydrogen sulfide (H_2S) removal and biogenic S^0 recovery, with more than 200 installations worldwide ('THIOPAQ Biogas desulphurization,' 2018). Biogenic S^0 globules, generated by different strains of bacteria, are considered to be hydrophilic, with a structure made of orthorhombic S^0 crystals surrounded by a hydrated layer of long-chain polymers or polythionates (Kamyshny et al., 2009; Kleinjan et al., 2003). The chemical composition of biogenic S^0 globules and their small particle size (2–40 μm) affect the S^0 (bio)chemical reactivity and make it more bioavailable for microorganisms (Findlay et al., 2014).

These exclusive properties of biogenic S^0 have promoted its application as a fertilizer (FERTIPAQ, the Netherlands) and in metal recovery technologies (Florentino et al., 2015). Only in the last two years, biogenic S^0 has been suggested for denitrification applications (Di Capua et al., 2016) due to its bioavailable nature and the possibility to offer a more affordable and sustainable nutrient removal solution. In this line, a possible integrated solution combining desulfurization of biogas with nitrogen removal from wastewaters can become applicable in the future, enabling to upgrade the current wastewater treatment configurations on a novel water resource recovery facility, in agreement with the EU Action Plan for the Circular Economy. To do so, more research on the chemistry and microbiology behind the use of biogenic S^0 for NO_3^- and NO_2^- removal is required.

The present research aims to investigate the fundamental aspects of autotrophic denitrification with biogenic S^0 (ADBIOS) using high-strength NO_3^- and NO_2^- synthetic waters. The main objectives of this study were to: (i) perform a physico-chemical and elemental characterization of the biogenic S^0 used; (ii) enrich a microbial consortium capable of NO_3^- and NO_2^- reduction and concomitant oxidation of biogenic S^0 in batch; (iii) use the enriched microbial community to evaluate the kinetics of biogenic S^0-based autotrophic denitrification, denitritation, and simultaneous denitrification-denitritation in batch bioassays; and (iv) investigate the structure of the bacterial communities in the presence of NO_3^-, NO_2^- or both. The impact of this study for the design and scale-up of biogenic S^0-driven denitrification and denitritation systems is discussed.

2. Materials and methods

2.1. Source of biogenic S^0 and development of the biogenic S^0-oxidizing microbial consortium

The biogenic S^0 (Fertipaq BV, the Netherlands, purity > 99%, 11% moisture content) from the Thiopaq process (Paques BV, the Netherlands) was used as electron donor in the batch bioassays aimed at denitrification and denitritation. An activated sludge collected from the denitrifying tank of a municipal wastewater treatment plant (Cassino, Italy) was used as inoculum (10% v/v) in the batch bioassays. The biogenic S^0-based denitrifying bacterial cultures were enriched for 3.5 months in 125 ml serum bottles with a working volume of 100 ml. The bottles were fed with the basal medium and trace elements as reported by Kostrytsia et al. (2018). NO_3^- or NO_2^- were individually added to the serum bottles with an initial concentration of 240 mg N/l. To ensure the presence of an adequate concentration of biogenic S^0 for complete denitrification or denitritation, an excess S^0 was used to maintain an S:N (g/g) ratio of 3.76 (1.5 times higher than the stoichiometric value). $NaHCO_3$ was added as buffer and carbon source with a concentration of 2.0 g/l.

Each bottle was purged with helium gas for 3 min to exclude oxygen, prior to sealing the bottle with a rubber stopper and an aluminum crimp. Subsequently, the bottles were placed on a gyratory shaker at 300 rpm and temperature was maintained at 30 (± 2) °C by means of a water bath. The enrichment was subcultured when NO_3^--N or NO_2^--N concentrations approached zero. An enrichment was treated as 'stable' when the achieved denitrification or denitritation rates of the subcultures alternated by less than 5%.

2.2. Kinetic experiments

To knowledge of the authors, for the first time biogenic S^0-oxidizing microbial consortia capable of reducing NO_3^- or NO_2^- were developed. Three sets of batch bioassays were set up using the enriched biomass to investigate the kinetics of ADBIOS, i.e. denitrification (A: NO_3^- and S^0), denitritation (B: NO_2^- and S^0) and simultaneous denitrification-denitritation (C: NO_2^-, NO_3^- and S^0). The initial NO_3^- or NO_2^- concentrations were similar (i.e. 5% difference) to those used in a previous batch study on autotrophic denitrification with chemically synthesized S^0 (Kostrytsia et al., 2018). In the first experiment (A), batch bioassays were conducted to investigate the denitrification characteristics (NO_3^--N reduction rate, NO_2^--N accumulation and NO_2^--N reduction rates). During the second set of the experiments (B), NO_2^--N was used as the sole electron acceptor in order to evaluate the denitritation kinetics (NO_2^--N reduction rate) and assess the impact of biomass acclimation to NO_2^--N degradation. The simultaneous denitrification-denitritation experiment (C) was performed to study the effect of NO_3^--N on NO_2^--N degradation.

At the beginning of each experiment, the required amount of NO_3^--N and NO_2^--N from stock solutions was added into the serum bottles to achieve the desired initial concentration as reported in Table 1. Biogenic S^0, $NaHCO_3$, the basal medium and trace elements solution were supplied at the same concentrations as in the enrichment phase. Each serum bottle was inoculated with an enriched culture with an amount of approximately 217.5 (± 2.5) mg/l of volatile suspended solids (VSS). Abiotic controls were used to monitor the possible chemical reactions involving the electron donor and electron acceptor. Controls without electron donor (biogenic S^0) or electron acceptor (NO_3^- or NO_2^-) were carried out to estimate their possible degradation not associated with S^0-driven denitrification or denitritation. In each experiment, the denitrification and denitritation rates were calculated from the slope of the curve describing NO_3^--N and NO_2^--N degradations, respectively, versus time and expressed as mg NO_x^--N/l·d. The biomass specific denitrification and denitritation activities (mg NO_x^--N/g VSS·d) were calculated by normalizing the denitrification and denitritation rate data with the initial biomass concentration (g VSS/l).

2.3. Sampling and analytical techniques

The liquid samples were taken twice a day and stored at −20 °C prior to analysis. NO_3^-, NO_2^- and sulfate (SO_4^{2-}) concentrations were determined by ion chromatography, as reported elsewhere (Kiskira et al.,

Table 1
Design of batch experiments to investigate the kinetics of autotrophic denitrification (NO_3^--N and S^0), denitritation (NO_2^--N and S^0) and simultaneous denitrification-denitritation (NO_2^--N, NO_3^--N and S^0) at 30 (± 2) °C with biogenic S^0 as an electron donor and an S:N (g/g) ratio of 3.76.

Experiment	Initial concentration (mg/l)					pH
	NO_2^--N	NO_3^--N	Total N	S^0	VSS	
A: Denitrification (NO_3^- and S^0)	15	225	240	850	220[a]	8.7 ± 0.1
B: Denitritation (NO_2^- and S^0)	240	–	240	850	215[b]	8.9 ± 0.1
C: Denitrification and denitritation (NO_2^-, NO_3^- and S^0)	110	70	180	680	220[a]	8.8 ± 0.1
NO_3^-- and NO_2^--free controls	–	–	–	850	220[a]	8.8 ± 0.1
	–	–	–	850	215[b]	8.8 ± 0.1
S^0-free controls	–	240	240	–	220[a]	8.9 ± 0.1
	240	–	240	–	215[b]	8.9 ± 0.1
Abiotic controls	–	240	240	850	–	8.9 ± 0.1
	240	–	240	850	–	8.9 ± 0.1

[a] Microbial source: biomass enriched on NO_3^--N and S^0.
[b] Microbial source: biomass enriched on NO_2^--N and S^0.

2017b). Elemental S^0 was determined by reversed-phase chromatography as originally described by Kamyshny et al. (2009). In this study, a high-performance liquid chromatography (HPLC) system (Prominence LC-20A Series, Shimadzu, Japan) equipped with a Kinetex LC column (C18, 5100 Å) and a UV/Vis detector (SPD-20A, Shimadzu, Japan) at 230 nm was used to quantify elemental S^0. Prior to and at the end of the batch kinetic experiments, total suspended solids (TSS) and VSS of the liquid samples were determined according to the Standard Methods (APHA, 2011).

Laser size particle analysis (LSPA) was performed to determine the particle size distribution (PSD) of the raw and freeze-dried biogenic S^0 in a deionized water by a Mastersizer 2000 (Malvern Instruments, UK) laser diffraction particle sizer equipped with a HydroG sample dispersion wet unit. The measurement range of the instrument was from 0.02 to 2000 µm. Size parameters of the diameters $d_{0.1}$, $d_{0.5}$ and $d_{0.9}$ were presented with 10%, 50% and 90%, respectively, of the volume of the particles below the given number.

To investigate the chemical and structural origin of biogenic S^0, Raman spectra were obtained at random positions on the biogenic S^0 material using a Horiba LabRAM II Raman spectrometer (Horiba Jobin-Yvon, France). The instrument was equipped with a 600 groove·mm^{-1} diffraction grating, a confocal optical system, a Peltier-cooled CCD detector and an Olympus BX41 microscope arranged in 180° back-scatter geometry. The measurements were performed using a 532 nm laser channeled through a Leica L100X/0.75 objective, providing a laser spot diameter of ~1.5 µm.

Inductively coupled plasma mass spectrometry (ICP-MS) was used to determine quantifiable trace metals in biogenic S^0. The biogenic S^0 samples were freeze-dried at −52 °C (Freezone 12, Labconco, USA), and approximately 0.1 g of sample was digested with an optimized microwave digestion procedure (Anton Paar Multiwave 3000, Austria) using 3 ml of trace metal grade 67–69% HNO_3 (*ROMIL-SpA*™, USA) and 3 ml of 30% H_2O_2 (*Trace*SELECT® Ultra ≥ 30%, Sigma Aldrich, Germany) (Healy et al., 2016). The digested samples were transferred into trace metal-free centrifuge tubes (Labcon, Petaluma, USA), and elemental concentrations were determined using a PerkinElmer ELAN DRCe ICP-MS (Perkin Elmer, USA) using both standard and dynamic reaction cell (DRC) mode with methane as the carrier gas (Ratcliff et al., 2016) in a class1000 (ISO class 6) clean room.

2.4. Microbial community analysis

2.4.1. DNA extraction and high-throughput sequencing

The total genomic DNA was extracted from the inoculum (Section 2.1) and the biomass at the beginning and at the end of the experiments (Table 1) in triplicate, following the protocol described by Griffiths et al. (2000). A high-throughput sequencing of partial 16S rRNA gene on DNA samples was conducted by the Illumina MiSeq sequencing service (FISABIO, Spain). The primers 515F and 806R were applied to target the 16S rRNA gene. The raw sequence files supporting the results of this article are available in the European Nucleotide Archive under the project accession number PRJEB27906.

2.4.2. Bioinformatics

The abundance table was generated by constructing operational taxonomic units (OTUs). Initially, the paired-end reads were pre-processed as described by Schirmer et al. (2015). Briefly, the paired-end reads were trimmed and filtered using *Sickle v1.200*. Then, PANDAseq v2.4 was used to assemble the forward and reverse reads into a single sequence spanning the entire V4 region. This resulted in consensus sequences for each sample on which *VSEARCH v2.3.4* was used for OTU construction. The preprocessed reads from each sample were pooled together while barcodes were added. The reads were then dereplicated and sorted in order of decreasing abundance (Schirmer et al., 2015). Subsequently, the reads were clustered based on 97% similarity, followed by a removal of clusters (*vsearch*). Finally, the OTU table was generated by matching the original barcoded reads against clean OTUs (a total of 1104 OTUs for n = 19 samples) at 97% similarity. The representative OTUs were taxonomically classified against the SILVA SSU Ref NR v123 database. Multisequence aligned the OTUs and used them with *FastTree v2.1.7* to generate the phylogenetic tree in *NEWICK* format. The biom file for the OTUs was then generated by combining the abundance table with the taxonomy information using *Qiime* workflow.

2.4.3. Statistical analysis

Statistical analyses were performed in *R v3.4.4* using the combined data generated from the bioinformatics as well as meta data associated with the study. The *vegan* package was used for alpha and beta diversity analyses. For alpha diversity measures, the following indexes were calculated: *rarefied richness* – the estimated number of species after rarefying the abundance table to minimum library size; *Shannon entropy* – a commonly used index to measure balance within a community. The ordination of the OTU table in a reduced space was done using Principal Coordinate Analysis (PCoA) plots of OTUs using two different distance measures: *Bray-Curtis* distance metric which considered OTU abundance counts and; *Weighted Unifrac* distance that combined the phylogenetic distances weighted with relative abundances. Phylogenetic distances within each sample were further characterized by calculating the nearest taxa index (NTI) and net relatedness index (NRI) (Kembel et al., 2010). This analysis helped to determine whether the community structure was stochastic (driven by competition among taxa) or deterministic (driven by environmental pressure).

Sparse Projection to Latent Structure – Discriminant Analysis (sPLS-DA) was performed with the R's mixOmics package (Rohart et al., 2017). The procedure constructed artificial latent components of the predicted variables (OTU table collated at genus level) and the response variables by factorizing these matrices into *scores* and *loading vectors* in a new space such that the covariance between the scores of these two matrices in this space was maximized. The loading vector was constructed with the coefficients indicating the importance of each variable to define the component, i.e. non-zero coefficients in the loading vectors indicated the genera that vary significantly between the categories and were thus deemed as discriminants (Rohart et al., 2017). Fine tuning of the algorithm was applied by splitting the data into training and testing sets and then finding the classification error rates, employing two metrics, i.e. overall error rates and balanced error rates (BER).

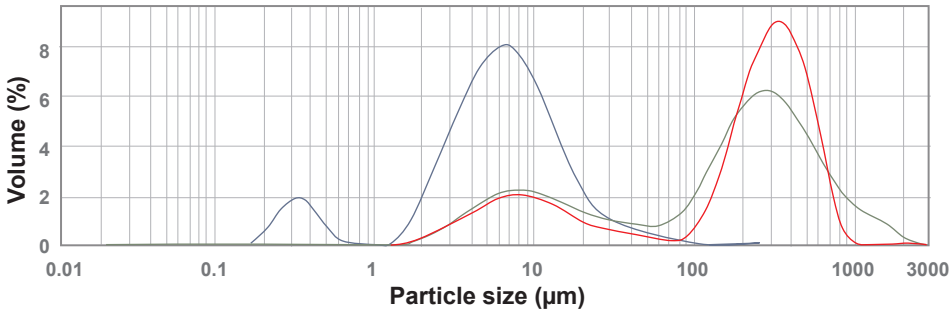

Fig. 1. Particle size distribution (PSD) of raw (—), freeze-dried (—) and raw biogenic S^0 after mixing (300 rpm, Time = 5 min, 30 °C) in water (—).

Table 2
Quantifiable trace metals in biogenic S^0 detected using ICP-MS (averages ± standard deviation; n = 3).

Element	Value (± SD) (µg g^{-1})	Element	Value (± SD) (µg g^{-1})	Element	Value (± SD) (µg g^{-1})
Al	5.11 ± 0.97	Ni	1.04 ± 0.10	Cr	9.63 ± 0.23
Ti	0.89 ± 0.13	Cu	6.79 ± 0.32	Fe	129.05 ± 5.21
Mn	4.19 ± 0.20	Mo	2.11 ± 0.06	Zn	19.69 ± 1.34
Co	2.78 ± 0.11	Ba	0.61 ± 0.04		

3. Results and discussion

3.1. Physico-chemical and elemental characterization of biogenic S^0

The PSD of biogenic S^0 is shown in Fig. 1. The raw biogenic S^0 sample consisted of particles with a median size of 241.16 µm and the 10% (6.88 µm) and 90% (508.89 µm) as measures of variability (Fig. 1). A surface weighted mean of 24.78 µm was quantified, which estimated the average diameter based on the surface area. In contrast, in previous studies on chemically synthesized S^0-based denitrification, the S^0 particle size was between 500 and 16000 µm (Christianson and Summerfelt, 2014; Sahinkaya et al., 2014; Sahinkaya and Kilic, 2014), which is approximately two orders of magnitude higher than that of the S^0 used in the current study.

To evaluate the degree of agglomeration of the biogenic S^0 and its behavior in suspension, the size distribution of the S^0 particles was also determined after mixing them in water (5 min at 300 rpm and 30 °C). The measured particles were with the median size of 4.69 µm and variability of the 10% (1.37 µm) and 90% (12.8 µm). This shows that the particle size of the biogenic S^0 was of the same order of magnitude of the S^0 particles (up to 1 µm) produced by sulfide-oxidizing bacteria in aqueous environment (Findlay et al., 2014). The contact of biogenic S^0 with water under mixing (i.e. 300 rpm) was likely to break sulfur agglomerations (Fig. 1). This could be explained by the hydrophilic surface of biogenic S^0, which hinders the particle-aggregation in water (Kleinjan et al., 2003). In contrast, chemically produced S^0 is more hydrophobic and aggregates quickly in aqueous solutions (Findlay et al., 2014).

The specific surface area (SSA) of elemental S^0 particles is a main driver for its biooxidation rate, including oxidation coupled to denitrification and denitritation (Kostrytsia et al., 2018). In previous studies, the higher reactivity of biogenic S^0 was attributed not only to its unique surface characterization, but also to a higher SSA associated with a smaller particle size compared to that of the chemically produced S^0 (Kleinjan et al., 2003). In this study, the small biogenic S^0 grain size of 4.69 µm obtained after mixing provided a high SSA of 3.38 m^2/g, compared to that of raw biogenic sulfur that had a 0.242 m^2/g SSA corresponding to a 241.16 µm grain size. In addition, the results of LSPA (Fig. 1) and Raman spectroscopy (data not shown) confirmed that the biogenic S^0 used in this study is an elemental microcrystalline orthorhombic sulfur. These findings are in line with a previously proposed biogenic model of a microcrystalline solid elemental sulfur covered by biopolymers (Janssen et al., 1999). Therefore, the microcrystallinity of biogenic S^0 particles results in its higher reactivity and solubility, as suggested by Pasteris et al. (2001).

During denitrification, the reactions of NO_3^- or NO_2^- reduction to nitrogenous oxides are catalyzed by metalloenzymes (Shao et al., 2010). Among the quantifiable trace metals detected in biogenic S^0 (Table 2), copper (Cu), molybdenum (Mo) and iron (Fe) are co-factors of metalloenzymes (Shao et al., 2010). Nitrite reductase (*NiR*) and nitrous oxide reductase (N_2OR) enzymes contain Cu. Mo is covalently attached to the protein in nitrate reductase (*NaR*), and Fe is cofactor for nitric oxide reductase (*NOR*). Additionally, Fe-S proteins, so-called ferredoxins, mediate electron transfer during NO_3^- and nitric oxide (NO) reduction (Shao et al., 2010). Thus, the supply of trace metals is essential for the high performance of denitrification and denitritation, and biogenic S^0 can effectively provide the necessary trace metals during these processes (Table 2). The possible inhibitory effect of heavy metals released by biosulfur on the activity of denitrifying biomass can be taken into consideration in a future study.

3.2. Effect of electron acceptor on ADBIOS kinetics

The evolution of pH, NO_3^--N, NO_2^--N and SO_4^{2-}-S concentrations as well as the remaining S^0 throughout the 2-week batch experiments is shown in Fig. 2. In the denitrification experiment (Fig. 2a and d), the achieved degradation rate of 49.4 mg NO_3^--N/l·d allowed the complete NO_3^- degradation in 14 days with a final biomass concentration of 450 mg VSS/l. The NO_3^--N removal efficiency reached up to 84% after the first 5 days, with NO_2^--N accumulating up to 135 mg/l. The NO_2^- accumulation was most likely ascribed to a higher enzyme activity of *NaR* compared to *NiR*, as also reported elsewhere (Du et al., 2016; Sun and Nemati, 2012). The high NO_2^--N build-up was followed by a drop of the NO_3^--N degradation rate to 7.8 mg/l·d from day 5 onwards. This was likely due to the inhibition of a NO_2^--N concentration above 60 mg/l on the activity of the denitrifying biomass (Guerrero et al., 2016).

In the denitritation experiments, the potential of the biogenic S^0-oxidizing biomass enriched on NO_2^- to reduce high NO_2^- concentrations was investigated (Fig. 2b and e). The bacteria were capable of completing NO_2^--N removal with the rate of 73.0 mg NO_2^--N/l·d, which resulted in a biomass growth up to 430 mg VSS/l. No detrimental effects were observed on denitritation at a NO_2^--N concentration as high as 240 mg/l. Additionally, the kinetics of simultaneous denitritation-denitrification were investigated in the presence of high NO_2^--N concentrations and microbial community enriched on NO_3^- (Fig. 2c). During the experiment, the highest NO_2^--N and NO_3^--N removal rates were 31.3 and 21.8 mg/l·d, respectively. The final biomass concentration in simultaneous denitritation-denitrification experiments was 320 mg VSS/l. Thus, the presence of NO_3^--N did not result in an inhibition of the *NiR* activity.

A higher accumulation of NO_2^--N and its slow degradation are generally observed when using chemically synthesized S^0 as electron donor for denitrification due to the low solubility of the S^0-based

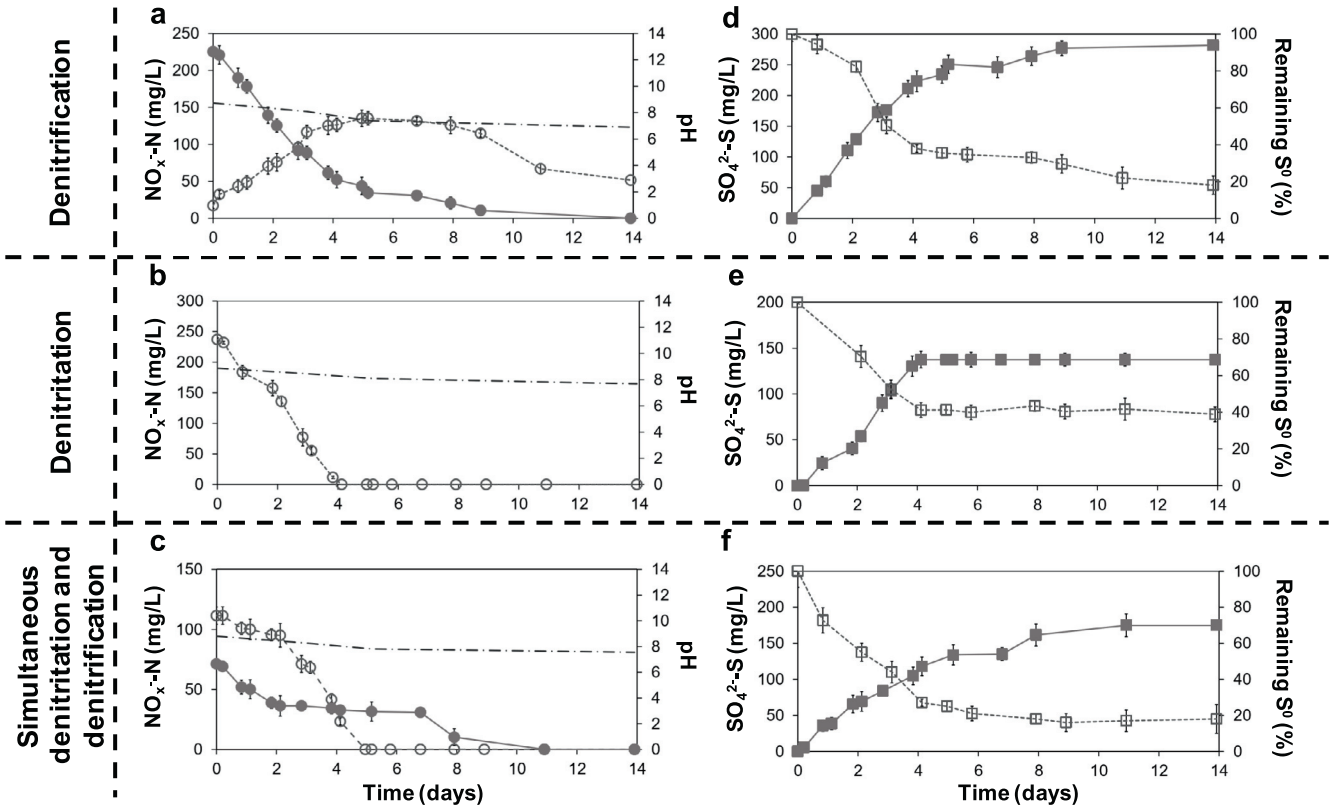

Fig. 2. Kinetics of denitrification (a, d), denitritation (b, e), and simultaneous denitritation-denitrification (c, f) coupled to biogenic S^0 oxidation in batch experiments using NO_3^--N, NO_2^--N and NO_3^--N with NO_2^--N, respectively, at 30 (± 2) °C and pH of 8.8 (± 0.2): NO_2^--N (○), NO_3^--N (●) and pH ( ) evolution is shown in a), b) and c), while SO_4^{2-}-S (■) concentration and the remaining biogenic S^0 (□) are shown in d), e) and f).

substrate (Sahinkaya et al., 2015; Simard et al., 2015). As the microcrystallinity and hydrophilic properties (Section 3.1) provided a higher bioavailability of biogenic S^0, a faster degradation of the accumulated NO_2^--N (20.9 mg NO_2^--N/l·d) during denitrification was achieved (Fig. 2a and c). Even a higher NO_2^--N degradation rate (73.0 mg NO_2^--N/l·d) could be obtained by using the biomass enriched on NO_2^- (Fig. 2b). Therefore, the use of NO_2^- acclimated biomass is recommended for biogenic S^0-driven denitrification treating high-strength NO_3^- wastewaters to control the high NO_2^--N accumulation.

SO_4^{2-}-S was the only sulfur product of the biogenic S^0 oxidation (Fig. 2 and f). This observation was confirmed by the stochiometric consumption of the biogenic S^0 with NO_3^--N or NO_2^--N (Sun and Nemati, 2012). No denitrification and denitritation were observed in the abiotic and electron donor-free controls (data not shown). In this study, specific denitrification and denitritation activities of 223.0 mg NO_3^--N/g VSS·d and 339.5 mg NO_2^--N/g VSS·d, respectively, were achieved by the biogenic S^0-oxidizing microbial consortium (Table 3). The high solubility of biogenic S^0, which was likely attributed to the hydrophilic properties and the lower particle size of the biogenic S^0 particles (Section 3.1), induced a significantly higher NO_2^--N degradation (Fig. 2a). The kinetics of ADBIOS (including both denitrification and denitritation) was characterized by 10-time higher rates compared to those obtained with chemically synthesized S^0 (Kostrytsia et al., 2018), with both studies being performed at similar initial NO_3^- and NO_2^- concentrations.

Table 3
The highest denitrification and denitritation rates obtained with different S^0 sources as electron donor by a 3.5-month enriched biomass at initial concentrations of 225.0 and 240.0 mg/l for NO_3^--N and NO_2^--N, respectively, and 220 and 215 mg VSS/l in denitrification and denitritation experiments with biogenic S^0, respectively, and 1000 mg VSS/l in experiments with chemically synthesized S^0 (Kostrytsia et al., 2018).

Electron acceptor		Biogenic S^0	Chemically synthesized S^0 (Kostrytsia et al., 2018)
NO_3^-	Denitrification rate (mg NO_3^--N/l·d)[a]	49.4	20.9
	Specific denitrification activity (mg NO_3^--N/g VSS·d)[a]	223.0	20.9
NO_2^-	Denitritation rate (mg NO_2^--N/l·d)[b]	73.0	10.7
	Specific denitritation activity (mg NO_2^--N/g VSS·d)[b]	339.5	10.7

[a] Biomass enriched for 3.5 months on NO_3^--N and S^0.
[b] Biomass enriched for 3.5 months on NO_2^--N and S^0.

3.3. Effect of different electron acceptors on microbial communities performing ADBIOS

The efficiency of biological NO_3^- and NO_2^- reduction depends on the community composition of microorganisms (Shao et al., 2010). Thus, the genera prevailing under each experimental condition (Fig. 3a), i.e. denitrification (A), denitritation (B) and simultaneous denitritation-denitrification (C) at the beginning (T_0) and at the end (T_F) of the experiments, as well as the microbial community of the raw activated sludge (AS) used as inoculum, were analyzed in this study (Figs. 3 and 4).

The enrichment in both denitrification (A) and simultaneous denitrification-denitritation (C) (i.e. NO_3^- and NO_2^- both involved) led to similar microbial communities with samples A T_F and C T_F clustering closer to each other on the PCoA plots (Fig. 3d). In contrast, when denitritation was performed alone (B) (i.e. with the sole NO_2^- involved), a distinct community was formed (B T_F) (Fig. 3d). Thus,

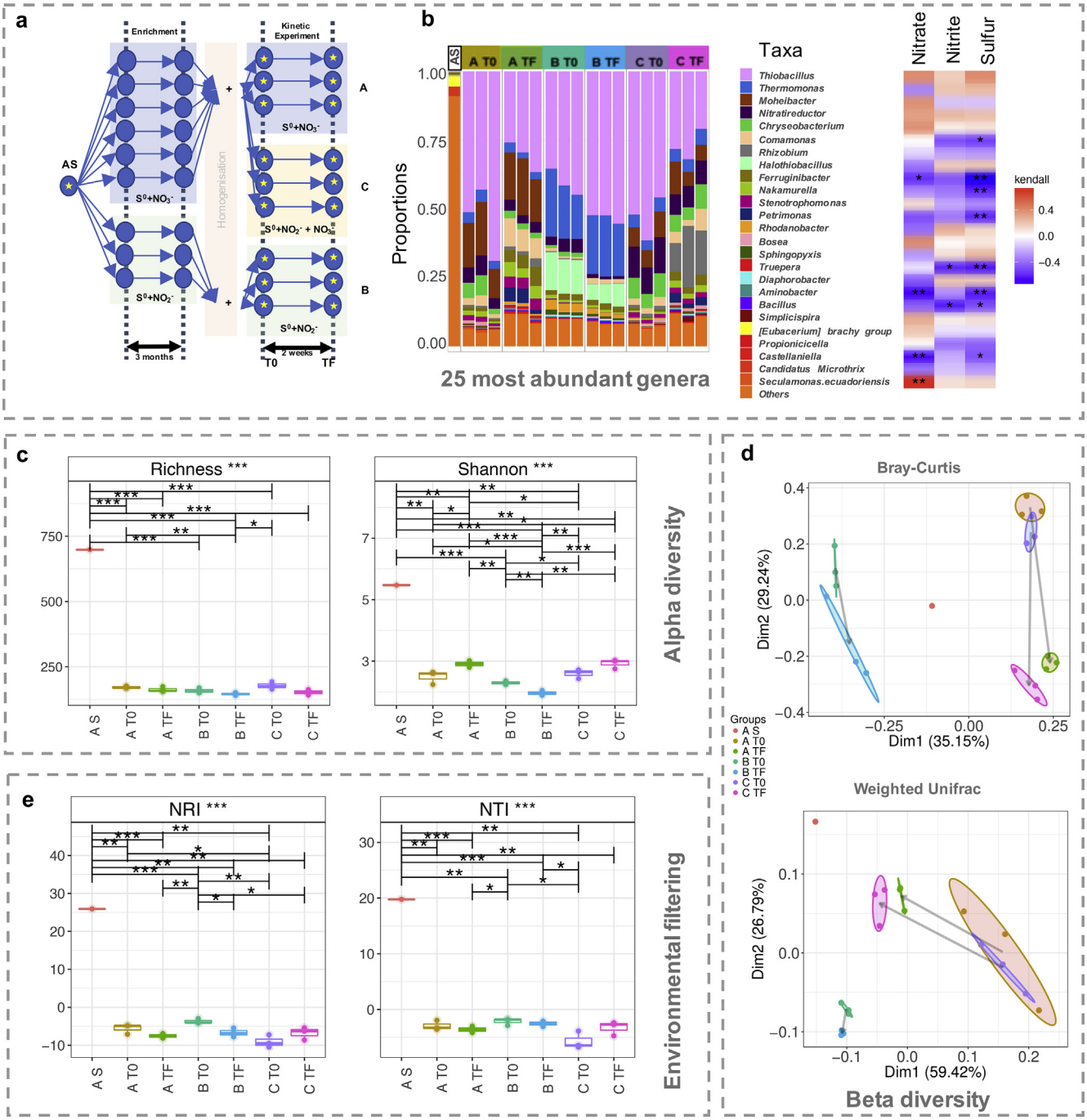

Fig. 3. a) The sampling points used for microbial community analysis: activated sludge (AS) used as inoculum, and samples at the beginning (T_0) and at the end (T_F) of the denitrification (A), denitritation (B) and simultaneous denitritation-denitrification (C) experiments. b) Taxa plots with the relative abundances of the 25 most abundant genera and their correlation with the environmental data; c) Alpha diversity metrics; d) PCoA of community data using Bray-Curtis distance and Weighted Unifrac dissimilarity; e) Stochastic vs deterministic nature of communities using NRI and NTI.

different key representative genera are selected when both (A and C) or only one electron acceptor (B) are used, with the former enriching for *Petrimonas*, *Bacillus*, *Truepera*, *Ferruginibacter*, *Castellaniella*, *Aminobacter* and the latter comprising of *Comamonas*, *Truepera*, *Bacillus* and *Clostridium sensu stricto 13*, based on taxa differential analysis (Fig. 3b). Some members of the genera *Comamonas* and *Bacillus* have been shown to be involved in NO_3^- reduction (Park and Yoo, 2009; Zhang et al., 2015), while in this study these were also abundant in the denitritation (B) experiment.

Additionally, in the top 25 most abundant genera *Thiobacillus* and *Moheibacter* were predominantly selected for the conditions with two electron acceptors (A and C) (Fig. 3b). In contrast, the condition with one electron acceptor (B) selected for different communities predominantly (~75%) comprising of *Thiobacillus* and *Thermomonas* (Fig. 3b). *Thiobacillus* has been reported as ubiquitous in denitrification applications with reduced sulfur compounds, e.g. particulate chemically synthesized S^0 and soluble $S_2O_3^{2-}$ (Di Capua et al., 2016; Kostrytsia et al., 2018) and is capable of withstanding high NO_2^- concentrations (Chen et al., 2018; Gao et al., 2017; Zhang et al., 2015), as also observed in this study with hydrophilic biosulfur (Fig. 2b). The recently isolated species within the *Moheibacter* genus were not yet reported to perform NO_2^- reduction (Schauss et al., 2016).

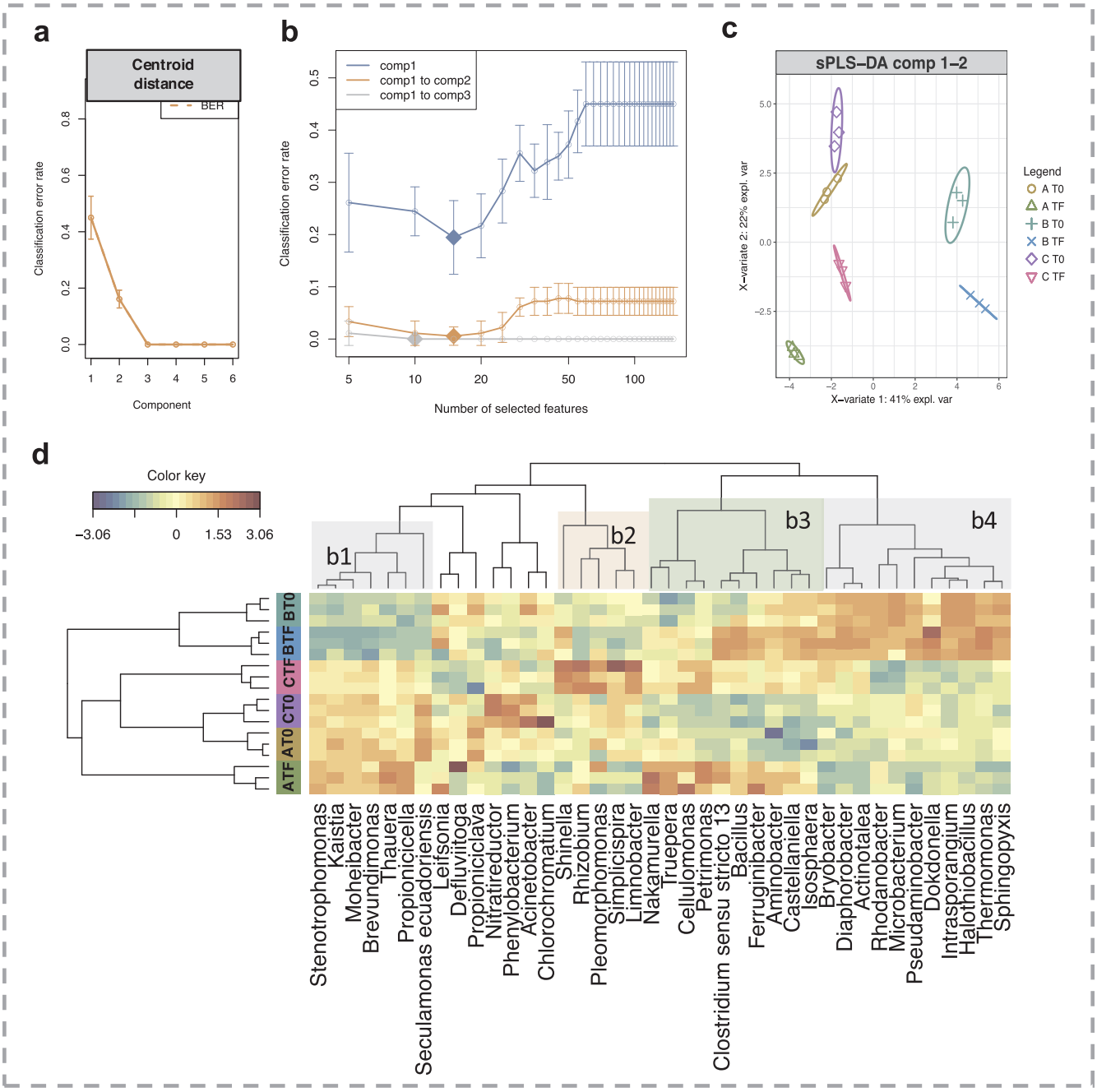

Fig. 4. a) The number of latent components for genera table after evaluating the performance of the PLS-DA algorithm. b) The number of discriminating features in each of 3 components with minimum classification error rates. c) Color-coded clustered image map of the discriminating genera with the hierarchical agglomeration clustering on rows and columns shown as dendrograms.

Following the sPLS-DA algorithm, only 40 genera were varying between the conditions in the kinetic experiments (Fig. 4a-c). The communities, when two (A and C) or one electron acceptor (B) were used, mainly differed in terms of genera represented by *Strenotrophomonas*, *Kaistia*, *Moheibacter*, *Brevundimonas*, *Thauera*, *Propionicicella*, *Seculamonas ecuadoriensis* (**block b1**); and *Bryobacter*, *Diaphorobacter*, *Actinotalea*, *Rhodanobacter*, *Microbacterium*, *Pseudaminobacter*, *Dokdonella*, *Intrasporangium*, *Halothiobacillus*, *Thermomonas*, and *Sphingopyxis* (**block b4**). **Block 1** was under expressed in denitritation (B), whereas **block b4** was over expressed in denitritation (B), and vice versa for denitrification (A) and simultaneous denitrification-denitritation (C). Similarly, *Strenotrophomonas*, *Thauera*, *Diaphorobacter* and *Halothiobacillus* were also reported in denitrifying reactors with chemically synthesized S^0 (Xu et al., 2015; Zhang et al., 2015). *Rhodanobacter*, *Dokdonella* and *Thermomonas* genera within the *Xanthomonadaceae* family are capable of using organic products from cell lysis to fuel denitrification (Xu et al., 2015). *Pseudaminobacter* is capable to oxidize reduced sulfur compounds directly to SO_4^{2-} (Ghosh and Dam, 2009).

The co-presence of the two electron acceptors mainly selected for (Fig. 4d): *Shinella*, *Rhizobium*, *Pleomorphomonas*, *Simplicispira*, *Limnobacter* (**block b2**); and *Nakamurella*, *Truepera*, *Cellulomonas*, *Petrimonas*, *Clostridium sensu stricto 13*, *Bacillus*, *Ferruginibacter*, *Aminobacter*, *Castellaniella*, *Isosphaera* (**block b3**). *Shinella, Rhizobium*, *Simplicispia* and *Limnobacter* were detected in reactors with reduced sulfur compounds treating NO_3^- pollution (Christianson et al., 2015; Zhang et al., 2015).

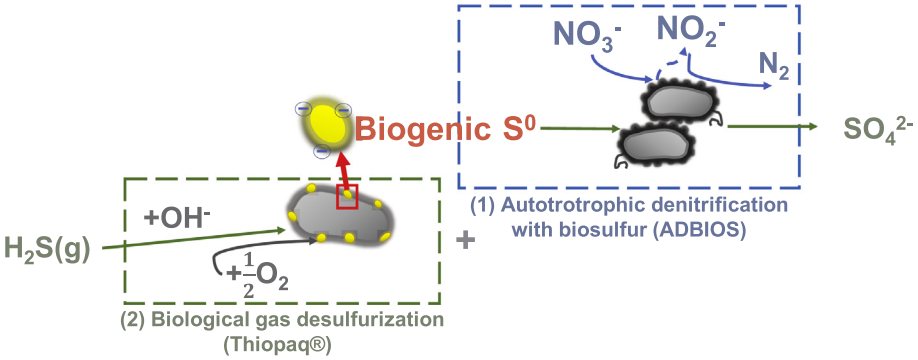

Fig. 5. Integrated ADBIOS (1) with NO_3^- and NO_2^- used as electron acceptors and biological gas desulfurization Thiopaq® (2).

The *Nakamurella, Truepera, Petrimonas, Clostridium sensu stricto 13*, *Bacillus*, *Ferruginibacter Aminobacter*, *Castellaniella, Isosphaera* genera are known to comprise of some denitrifying bacteria (He et al., 2018; Zhao et al., 2016). In addition, looking at **block b3**, the right tree comprising *Clostridium sensu scricto 13*, *Bacillus*, *Ferruginibacter*, *Aminobacter*, *Castellaniella*, and *Isosphaera* is overexpressed for both denitritation (B) and denitrification (A), indicating that those genera can degrade NO_2^- (Park and Yoo, 2009; Spain and Krumholz, 2012; Xu et al., 2017).

3.4. Opportunities for ADBIOS as a part of a sustainable and integrated wastewater treatment system

ADBIOS (Fig. 5 [1]) provides a sustainable technological solution for biological nitrogen removal fueled by biogenic S^0, as a by-product of biogas desulfurization (Fig. 5 [2]). The benefits of the process, such as a 10-time faster kinetics (Section 3.2) compared to that of autotrophic denitrification with chemically synthesized S^0, make it technologically attractive and economically feasible. In addition, the high NO_2^- degradation rate in the presence of a NO_2^--enriched biomass suggests that ADBIOS can also be applied for NO_2^- removal from wastewaters (Fig. 5 [1]). Generally, ADBIOS implements the reuse of a waste resource (S^0) into conventional nitrogen removal systems and creates a potential for an integrated process combining wastewater and flue gas treatment. Therefore, the scale-up of ADBIOS is of a great interest, and the current study can serve as the basis of the necessary fundamental information on the process. However, not each site may have readily-available biogenic S^0 supply, and biosulfur transportation might be required, which needs to be considered within an economic balance.

4. Conclusions

The biogenic S^0-oxidizing microbial consortia capable of reducing NO_3^- or NO_2^- mostly included *Thiobacillus*, *Moheibacter* and *Thermomonas*. The biogenic S^0 showed an orthorhombic crystalline structure, having a 4.69 µm median particle size and a 3.38 m^2/g SSA, which made it particularly reactive and bioavailable. The specific denitrification and denitritation activities as high as 223.0 mg NO_3^--N/g VSS·d and 339.5 mg NO_2^--N/g VSS·d, respectively, resulted in enhanced denitrification and denitritation rates compared to those of chemically synthesized S^0. Moreover, the use of biogenic S^0 induced a lower accumulation of NO_2^-, alleviating the activity of the denitrifying consortia.

Acknowledgments

This work was supported by the Marie Skłodowska-Curie European Joint Doctorate (EJD) in Advanced Biological Waste-To Energy Technologies (ABWET) funded by the Horizon 2020 program under the grant agreement no. 643071. Umer Zeeshan Ijaz is funded by a NERC Independent Research Fellowship (NE/L011956/1). The authors gratefully thank Fertipaq B.V. (the Netherlands), the daughter company of Paques B.V. (the Netherlands), for providing the biogenic sulfur.

Notes

The authors declare no competing financial interest.

References

APHA, 2011. Standard Methods for the Examination of Water and Wastewater.
Chen, F., Li, X., Gu, C., Huang, Y., Yuan, Y., 2018. Selectivity control of nitrite and nitrate with the reaction of S^0 and achieved nitrite accumulation in the sulfur autotrophic denitrification process. Bioresour. Technol. 266, 211–219.
Christianson, L., Lepine, C., Tsukuda, S., Saito, K., Summerfelt, S., 2015. Nitrate removal effectiveness of fluidized sulfur-based autotrophic denitrification biofilters for recirculating aquaculture systems. Aquac. Eng. 68, 10–18.
Christianson, L., Summerfelt, S., 2014. Fluidization velocity assessment of commercially available sulfur particles for use in autotrophic denitrification biofilters. Aquac. Eng. 60, 1–5.
Di Capua, F., Ahoranta, S.H., Papirio, S., Lens, P.N.L., Esposito, G., 2016. Impacts of sulfur source and temperature on sulfur-driven denitrification by pure and mixed cultures of *Thiobacillus*. Process Biochem. 51, 1576–1584.
Du, R., Peng, Y., Cao, S., Li, B., Wang, S., Niu, M., 2016. Mechanisms and microbial structure of partial denitrification with high nitrite accumulation. Appl. Microbiol. Biotechnol. 100, 2011–2021.
Findlay, A.J., Gartman, A., Macdonald, D.J., Hanson, T.E., Shaw, T.J., Luther, G.W., 2014. Distribution and size fractionation of elemental sulfur in aqueous environments: the Chesapeake Bay. Geochim. Cosmochim. Acta 142, 334–348.
Florentino, A.P., Weijma, J., Stams, A.J.M., Sánchez-Andrea, I., 2015. Sulfur reduction in acid rock drainage environments. Environ. Sci. Technol. 49, 11746–11755.
Gao, L., Zhou, W., Huang, J., He, S., Yan, Y., Zhu, W., Wu, S., Zhang, X., 2017. Nitrogen removal by the enhanced floating treatment wetlands from the secondary effluent. Bioresour. Technol. 234, 243–252.
Ghosh, W., Dam, B., 2009. Biochemistry and molecular biology of lithotrophic sulfur oxidation by taxonomically and ecologically diverse bacteria and archaea. FEMS Microbiol. Rev. 33, 999–1043.
Griffiths, R.I., Whiteley, A.S., Anthony, G., Donnell, O., Bailey, M.J., Donnell, A.G.O., 2000. Rapid method for coextraction of DNA and RNA from natural environments for analysis of ribosomal DNA- and rRNA-based microbial community composition. Appl. Environ. Microbiol. 66, 5488–5491.
Guerrero, L., Montalvo, S., Huiliñir, C., Campos, J.L., Barahona, A., Borja, R., 2016. Advances in the biological removal of sulphides from aqueous phase in anaerobic processes: a review. Environ. Rev. 24, 84–100.
He, S., Ding, L., Pan, Y., Hu, H., Ye, L., Ren, H., 2018. Nitrogen loading effects on nitrification and denitrification with functional gene quantity/transcription analysis in biochar packed reactors at 5 °C. Sci. Rep. 8, 1–9.
Healy, M.G., Ryan, P.C., Fenton, O., Peyton, D.P., Wall, D.P., Morrison, L., 2016. Bioaccumulation of metals in ryegrass (*Lolium perenne L.*) following the application of lime stabilised, thermally dried and anaerobically digested sewage sludge. Ecotoxicol. Environ. Saf. 130, 303–309.
Janssen, A.J.H., Lettinga, G., de Keizer, A., 1999. Removal of hydrogen sulphide from wastewater and waste gases by biological conversion to elemental sulphur Colloidal and interfacial aspects of biologically produced sulphur particles. Colloids Surf., A 151, 389–397.
Kamyshny, A., Borkenstein, C.G., Ferdelman, T.G., 2009. Protocol for quantitative detection of elemental sulfur and polysulfide zero-valent sulfur distribution in natural aquatic samples. Geostand. Geoanalytical Res. 33, 415–435.
Kembel, S.W., Cowan, P.D., Helmus, M.R., Cornwell, W.K., Morlon, H., Ackerly, D.D., Blomberg, S.P., Webb, C.O., 2010. Picante: R tools for integrating phylogenies and ecology. Bioinformatics 26, 1463–1464.
Kiskira, K., Papirio, S., van Hullebusch, E.D., Esposito, G., 2017a. Fe(II)-mediated autotrophic denitrification: a new bioprocess for iron bioprecipitation/biorecovery and simultaneous treatment of nitrate-containing wastewaters. Int. Biodeter. Biodeg. 119,

631–648.
Kiskira, K., Papirio, S., Van Hullebusch, E.D., Esposito, G., 2017b. Influence of pH, EDTA/Fe (II) ratio, and microbial culture on Fe (II)-mediated autotrophic denitrification. Environ. Sci. Pollut. Res. 24, 21323–21333.
Kleinjan, W.E., de Keizer, A., Janssen, A.J.H., 2003. Biologically produced sulfur. Top. Curr. Chem. 230, 167–188.
Kostrytsia, A., Papirio, S., Frunzo, L., Mattei, M.R., Porca, E., Collins, G., Lens, P.N.L., Esposito, G., 2018. Elemental sulfur-based autotrophic denitrification and denitritation: microbially catalyzed sulfur hydrolysis and nitrogen conversions. J. Environ. Manag. 211, 313–322.
Mora, M., Dorado, A.D., Gamisans, X., Gabriel, D., 2015. Investigating the kinetics of autotrophic denitrification with thiosulfate: modeling the denitritation mechanisms and the effect of the acclimation of SO-NR cultures to nitrite. Chem. Eng. J. 262, 235–241.
Paques, THIOPAQ. Biogas desulphurisation. http://en.paques.nl/products/featured/thiopaq. webpage visited July 2018.
Park, J.Y., Yoo, Y.J., 2009. Biological nitrate removal in industrial wastewater treatment: which electron donor we can choose. Appl. Microbiol. Biotechnol. 82, 415–429.
Pasteris, J.D., Freeman, J.J., Goffredi, S.K., Buck, K.R., 2001. Raman spectroscopic and laser scanning confocal microscopic analysis of sulfur in living sulfur-precipitating marine bacteria. Chem. Geol. 180, 3–18.
Ratcliff, J.J., Wan, A.H.L., Edwards, M.D., Soler-vila, A., Johnson, M.P., Abreu, M.H., Morrison, L., 2016. Metal content of kelp (*Laminaria digitata*) co-cultivated with Atlantic salmon in an Integrated Multi-Trophic Aquaculture system. Aquaculture 450, 234–243.
Rohart, F., Gautier, B., Singh, A., Le Cao, K.-A., 2017. mixOmics: an R package for 'omics feature selection and multiple data integration. PLoS Comput. Biol. 13, e1005752.
Sahinkaya, E., Kilic, A., 2014. Heterotrophic and elemental-sulfur-based autotrophic denitrification processes for simultaneous nitrate and Cr(VI) reduction. Water Res. 50, 278–286.
Sahinkaya, E., Kilic, A., Duygulu, B., 2014. Pilot and full scale applications of sulfur-based autotrophic denitrification process for nitrate removal from activated sludge process effluent. Water Res. 60, 210–217.
Sahinkaya, E., Yurtsever, A., Aktaş, Ö., Ucar, D., Wang, Z., 2015. Sulfur-based autotrophic denitrification of drinking water using a membrane bioreactor. Chem. Eng. J. 268, 180–186.
Schauss, T., Busse, H., Golke, J., Peter, K., Glaeser, S.P., 2016. *Moheibacter stercoris sp. nov.*, isolated from an input sample of a biogas plant. Int. J. Syst. Evol. Microbiol. 66, 2585–2591.
Schirmer, M., Ijaz, U.Z., Amore, R.D., Hall, N., Sloan, W.T., Quince, C., 2015. Insight into biases and sequencing errors for amplicon sequencing with the Illumina MiSeq platform. Nucleic Acids Res. 43, e37.
Shao, M.F., Zhang, T., Fang, H.H.P., 2010. Sulfur-driven autotrophic denitrification: diversity, biochemistry, and engineering applications. Appl. Microbiol. Biotechnol. 88, 1027–1042.
Simard, M.-C., Masson, S., Mercier, G., Benmoussa, H., Blais, J.-F., Coudert, L., 2015. Autotrophic denitrification using elemental sulfur to remove nitrate from saline aquarium waters. J. Environ. Eng. 141 04015037.
Spain, A.M., Krumholz, L., 2012. Cooperation of three denitrifying bacteria in nitrate removal of acidic nitrate- and uranium-contaminated groundwater. Geomicrobiol. J. 29, 830–842.
Sun, Y., Nemati, M., 2012. Evaluation of sulfur-based autotrophic denitrification and denitritation for biological removal of nitrate and nitrite from contaminated waters. Bioresour. Technol. 114, 207–216.
Wang, Y., Bott, C., Nerenberg, R., 2016. Sulfur-based denitrification: effect of biofilm development on denitrification fluxes. Water Res. 100, 184–193.
Xu, D., Xiao, E., Xu, P., Zhou, Y., He, F., Zhou, Q., Xu, D., Wu, Z., 2017. Performance and microbial communities of completely autotrophic denitrification in a bioelectrochemically-assisted constructed wetland system for nitrate removal. Bioresour. Technol. 228, 39–46.
Xu, G., Peng, J., Feng, C., Fang, F., Chen, S., Xu, Y., Wang, X., 2015. Evaluation of simultaneous autotrophic and heterotrophic denitrification processes and bacterial community structure analysis. Appl. Microbiol. Biotechnol. 99, 6527–6536.
Zhang, L., Zhang, C., Hu, C., Liu, H., Qu, J., 2015. Denitrification of groundwater using a sulfur-oxidizing autotrophic denitrifying anaerobic fluidized-bed MBR: performance and bacterial community structure. Appl. Microbiol. Biotechnol. 99, 2815–2827.
Zhao, H., Zhao, J., Li, F., Li, X., 2016. Performance of denitrifying microbial fuel cell with biocathode over nitrite. Front. Microbiol. 7, 1–7.
Zou, G., Papirio, S., Lakaniemi, A., Ahoranta, S.H., Puhakka, J.A., 2016. High rate autotrophic denitrification in fluidized-bed biofilm reactors. Chem. Eng. J. 284, 1287–1294.